Life Sciences 130 (2015) 66–72

Contents lists available at ScienceDirect

Life Sciences

journal homepage: www.elsevier.com/locate/lifescie

Neonatal androgenization-induced early endocrine–metabolic and ovary misprogramming in the female rat

Luisina Ongaro [a], Natalia R. Salvetti [b], Andrés Giovambattista [a], Eduardo Spinedi [c,*], Hugo H. Ortega [b]

[a] Neuroendocrine Unit (IMBICE, CONICET-CICPBA), La Plata, Argentina
[b] Institute of Veterinary Sciences (ICIVET-Litoral), UNL/CONICET, Santa Fe, Argentina
[c] Centre for Experimental & Applied Endocrinology (CENEXA, UNLP-CONICET La Plata), Argentina

ARTICLE INFO

Article history:
Received 24 December 2014
Received in revised form 8 March 2015
Accepted 10 March 2015
Available online 26 March 2015

Keywords:
Growth
Insulin
Adipose tissue
Leptin
Ovary
Steroidogenesis

ABSTRACT

Aim: Androgen excess predisposes the organism to develop metabolic–endocrine and reproductive dysfunctions, among them the development of a phenotype resembling that of human Polycystic Ovary Syndrome (PCOS).
Methods: We analyzed the impact of a single neonatal (5 day-old) testosterone propionate (TP; s.c. 1.25 mg/female pup) dose on: a) several metabolic–endocrine activities and b) ovarian steroidogenic and granulosa cell (GC) functions and also follicular population in juvenile and adult TP and control (CT) rats.
Key findings: Compared to CT rats, TP animals were characterized by: a) accelerated growth, hyperadiposity and hyperleptinemia, b) very early (pre-weaning age) vaginal opening, c) hyperinsulinemia in adult life, d) dysfunctional ovarian steroidogenesis, e) conserved GC functionality in both juveniles (*in vitro*) and adults (*in vivo*), and f) estrous cycles arrested at estrus. Finally, histological studies of the ovaries indicated that in TP (*vs.* CT) rats: i) primary and antral follicle frequencies were 3- and 15-fold higher and lower, respectively, in juveniles and ii) secondary and atretic follicle frequencies were 3- and 5-fold lower and higher, respectively, in adults. Large cystic images without corpus luteum were observed in the ovaries from adult TP rats only.
Significance: Our results strongly suggest that transient neonatal hyperandrogenemia induced early misprogramming of metabolic–endocrine and ovarian (steroidogenesis/folliculogenesis) functions. Conversely, TP rats preserved their ovary GC endocrine function. Our results further support the high risk of developing ovarian hyperstimulation syndrome for infertile women with transient/chronic hyperandrogenemia (PCOS) subjected to assisted reproductive technologies.

1. Introduction

A very common cause of menstrual disturbances, chronic anovulation and hyperandrogenism in pre-menopausal women is Polycystic Ovary Syndrome (PCOS) [9,10]. Although a very large population of women at reproductive age is affected by PCOS, diagnosis of this syndrome is still difficult for physicians [11]. Insulin resistance, with or without compensatory hyperinsulinemia, is frequently associated with PCOS [3,11,13]. Moreover, clinical and experimental studies suggest interaction between insulin and sex hormones in healthy subjects [2]. We previously found that androgenization in normal female rats, at either neonatal [1,19] or early post-pubertal [20] age, developed impaired insulin sensitivity in adulthood. We also observed a severe hypothalamic–pituitary–ovary (HPO) axis dysfunction in neonatally androgenized adult female rats. Indeed, on reaching adulthood, rats developed an altered pulsatile rhythm of gonadotropin secretion (*e.g.* decreased average mean values, decreased FSH peak amplitude values and increased LH:FSH ratio) and impaired *in vivo* LHRH-stimulated LH–FSH release [23]. These abnormalities have been ascribed to a neonatal hypothalamic effect of transient peripheral androgen excess (hypothalamic androgenization), later resulting in infertile individuals [4].

Regarding the relation between early hyperandrogenemia and adipose tissue function, we previously established that 100 day-old neonatal androgenized female rats are heavier and display greater adiposity, hyperleptinemia, impaired peripheral insulin sensitivity, and increased risk of developing dyslipidemia and cardiovascular risk [1]. In this regard, although physiological peripheral leptin levels are needed for normal HPO axis function [21], chronic high plasma leptin concentrations (leptin resistance) are critical for consequent ovary dysfunction (*e.g.* anovulation) [32]. Nevertheless, it is accepted that follicle oocytes and, granulosa and theca cells express androgen receptor, a gonadotropin-regulated element [28] that must be fine-tuned by appropriate androgen stimulation to assure normal follicle development and ovulation [28]. Tyndall et al. [24] recently investigated the effects of fetal and post-natal treatment with multiple high doses of androgen in female rats. These authors found that fetal injury (transient hyperandrogenemia in dams) failed to alter rat ovary folliculogenesis

* Corresponding author at: CENEXA (UNLP-CONICET), Argentina.
E-mail address: spinedi@cenexa.org (E. Spinedi).

http://dx.doi.org/10.1016/j.lfs.2015.03.008
0024-3205/

or fertility. The authors also claimed that multiple doses of androgen administered at any post-natal age (before 25 days of age) induced an incomplete PCOS rat phenotype [24].

In the present study, we aimed to investigate in the female rat whether a single, early post-natal (day 5), testosterone propionate (TP; 1.25 mg/pup, s.c.) treatment would be able to change the programming of metabolic–endocrine and reproductive functions. With this aim, we evaluated: a) several peripheral biomarkers and b) ovarian functionality (some steps of the steroidogenic process, folliculogenesis and granulosa cell endocrine function) in TP and their littermate control (CT) female rats when reaching juvenile and adult ages.

2. Materials and methods

2.1. Experimental animals

We used the classical Barraclough's animal model [4], previously validated in our laboratory [1]. Briefly, 5 day-old Sprague–Dawley female rat pups (10.65 ± 0.27 g BW; n = 80) were s.c. injected with 50 μL of sterile corn oil either alone (CT group; n = 35/40) or containing 1.25 mg of TP (Organon Lab., Argentina, n = 35/40). The vaginal opening was checked between 7 and 45 days of age. After weaning (21 days of age), rats were housed individually. Body weight (BW) and food intake were recorded daily (between 07:30 and 08:30 h) up to the corresponding experimental day (juvenile and adult ages, 30 and 60 days of age, respectively). Animals were kept in a light- (lights on from 07:00 to 19:00 h) and temperature (22 °C)-controlled room throughout the experiment. Rats were fed a commercial rat diet (Ganave Lab., Argentina) and provided with tap water *ad libitum* throughout the entire housing period. The experiments were approved by our Institutional Animal Care Committee; international regulations concerning ethical use of animals were strictly followed.

2.2. Experimental designs

Experiment 1. Rats from both groups were killed (between 08:00 and 09:00 h) at 30 days of age (juvenile age) in non-fasting conditions. Immediately after killing trunk blood was collected (into EDTA 10%–sodium fluoride coated plastic tubes), parametrial adipose tissue (PMAT) and ovaries were dissected, weighed, and either used for (see below) histological analyses or kept frozen (at −80 °C) until further assays.

Experiment 2. Individually caged rats (CT and TP) were injected (in the morning of days 27, 28 and 29 of age) s.c. daily with 1 mg of xenoestrogen [diethylstilbestrol (DES) dissolved in 100 μL of sterile corn oil] to stimulate the development of early antral follicles. Animals were killed the next morning (08:00–09:00 h; 30 days of age) and ovaries were immediately removed for granulosa cell (GC) isolation and culture. Briefly, GCs from DES-treated rats were isolated by ovary puncture (30-gauge needle) as described elsewhere [26] and incubated in Dulbecco Modified Eagle medium (DMEM, 4.5 g glucose/L)-Ham F12 (1:1, Gibco, Gaithersburg, MD, USA), EGTA (6.8 mM), and HEPES (10 mM; 15 min at 37 °C), then washed and incubated in DMEM-F12 (1:1), sucrose (0.5 M), and HEPES (10 mM; 5 min at 37 °C). After incubation, the medium was diluted with 2 volumes of DMEM-F12 and HEPES (10 mM), and ovaries were allowed to sediment. GCs were obtained by pressing ovaries between two pieces of nylon mesh (Nytex 50, Geneva, Switzerland). To eliminate contaminating theca/interstitial cells, the crude GC suspension was layered over a 40% Percoll solution in saline solution and centrifuged at 400 ×*g* for 20 min. The purified GC layer was aspirated from the top of the Percoll solution and resuspended in DMEM-F12 (1:1) containing sodium bicarbonate (2.2 g/L; pH: 7.4). Cells were seeded on P12 multiwell plastic plates (Nunc, Roskilde, Denmark) precoated with collagen at a density of 3.5×10^5 viable cells per well. Cells were kept at 37 °C in a 5% CO_2 atmosphere. After 3 h, media were changed to remove nonattached cells and replaced by fresh media containing antibiotics, delta-4-androstenedione (10^{-7} M) and 100 μL of fresh medium either alone or containing hCG (0.05–0.5 IU/mL). Cells were then cultured for 48 h. At the end of this period, media were removed and kept frozen (−20 °C) until measurement of 17β-estradiol (E2) concentrations (see below).

Experiment 3. Vaginal smears of rats from both groups were examined daily for three consecutive estrous cycles before experimentation [1]. Throughout this time period, samples obtained from TP rats indicated that they had attained constant estrus. Rats from both groups were then killed (between 08:00 and 09:00 h) on day 60 of age (adult age), at proestrous stage (CT) or arrested estrous stage (TP), in non-fasting condition. Immediately after killing, trunk blood was collected (into EDTA 10%–sodium fluoride coated plastic tubes) and ovaries were dissected and either used for histological analyses or kept frozen (at −80 °C).

Experiment 4. Vaginal smears of rats from both groups were examined daily for three consecutive estrous cycles before experimentation. On the morning (07:00–08:00 h) of the experimental day (age 60–61 days), CT (at the proestrus stage) and TP (at the arrested estrus stage) rats were i.v. implanted, under light phenobarbital anesthesia, to inhibit endogenous LH surge [30], with an indwelling catheter kept permeable by administering a small volume (100 μL) of vehicle (10 IU heparin/mL of sterile saline solution, containing 10 mg/mL bovine serum albumin). After recovery (10:00–11:00 h), rats were i.v. bled (a small volume, 200 μL) before (sample time zero) and 1 and 2 h after i.v. injection of 5 mIU/kg hCG (dissolved in 50 μL of vehicle, see above). Samples were rapidly centrifuged (at 4 °C, 15 min, 2600 ×*g*) and plasma samples kept frozen (−20 °C) until measurement of E2 concentrations.

2.3. Peripheral metabolite measurements

Circulating levels of leptin, insulin, total testosterone and corticosterone (Cort) were determined by specific radioimmunoassays (RIAs) as described earlier [1]. Plasma concentrations of 17-hydroxyprogesterone (17OHP4) were determined by a commercial RIA kit (Immunotech, France). Peripheral concentrations of triglyceride and glucose were determined by commercial enzymatic-colorimetric assays (Weiner Lab., Argentina). Finally, plasma and medium concentrations of E2 were determined by a specific RIA published and described in detail earlier [1]; the intra-assay coefficient of variation ranged between 4 and 8%, whereas the inter-assay coefficient of variation ranged between 9 and 12%.

2.4. Ovarian histology

For histological studies, five ovaries from each group were removed and immediately fixed in 4% paraformaldehyde (in 0.2 M pH 7.4 phosphate buffer), at 4 °C for a maximum of 3 days. Tissues were then washed with 0.01 M PBS, immersed in 70% ethanol for 24 h, embedded

in paraffin. Whole ovaries were then serially sectioned at 5 μm on a rotary microtome. To avoid duplicate analysis of follicles, five complete cross sections, 200 μm apart, were stained with hematoxylin–eosin. To prevent counting the same follicle twice [31], 4-μm step sections were mounted at 50-μm intervals onto microscope slides by the method described by Woodruff et al. [31]. For morphological analysis, sections were chosen as follows: five from each end and five from the middle of each ovary. Images were analyzed using the Image Pro-Plus 3.0.1 system (Media Cybernetics, Silver Spring, MA, USA) as described earlier [16]. Images at 100× magnification were digitalized with a Nikon DS-Fi1-U3 (Nikon, Japan) digital camera mounted on a conventional Nikon Eclipse 50i light microscope. Follicles were classified as follows: primary follicle, with one layer of cuboidal GCs; secondary follicle, with two or three layers of cuboidal GCs, without antral space; and antral follicle, with three or more layers of cuboidal GCs and one or more independent antral spaces. Follicles were considered atretic if they displayed two or more of the following criteria within a single cross section: more than ten pyknotic nuclei, GCs within the antral cavity, GCs pulling away from the basement membrane, or uneven GC layers [5]. The total number of follicles of five representative ovarian sections and the percentage (frequency) of follicles at different developmental stages were calculated and presented as the mean ± SEM.

2.5. RNA isolation and real-time quantitative PCR

Total RNA was isolated from the ovaries of rats of both groups by a modification of the single-step, acid guanidinium isothiocyanate–phenol–chloroform extraction method (TRIzol; Invitrogen, Life Tech., USA; cat. # 15596-026). The yield and quality of RNA extracted were assessed by a 260/280 nm optical density ratio and electrophoresis in denaturing conditions on 2% agarose gel. Total RNA (1 μg) was reverse-transcribed using random primers (250 ng) and Superscript III Rnase H-Reverse Transcriptase (200 U/μL Invitrogen, Life Tech, USA; cat # 18989-093). The primers applied for quantitative real-time PCR analyses are depicted in Table 1. Two microliters of the reverse transcription mix was amplified with the QuantiTect Syber Green PCR kit (Qiagen, cat. # 204143) containing 0.5 μM of each specific primer using the LightCycler Detection System (MJ Mini Opticon, Biorad). PCR efficiency was near 1. Threshold cycles (Ct) were measured in separate tubes in duplicate. Identity and purity of the amplified product were checked by electrophoresis on agarose mini-gels, and the melting curve was analyzed at the end of amplification. Values of the differences between the Ct were calculated in every sample for each gene of interest as follows: Ct of the gene of interest − Ct of the reporter gene, β-actin, whose mRNA levels did not differ between control and test groups, was the reporter gene. Relative changes in the expression level of one specific gene (ΔΔCt) were calculated as the ΔCt of the test group minus the ΔCt of the CT group, then presented as $2^{-\Delta\Delta Ct}$.

Table 1
Rat specific primers used for real-time PCR analyses were ACTB: β-actin; P450scc: cholesterol side-chain cleavage enzyme; P450c17: 17α-hydroxylase/17,20 lyase/17,20 desmolase enzyme; and CPY19: aromatase (se: sense; as: anti-sense; GBAN: **GenBank** Accession Number; amplicon length, in bp).

		GBAN	bp
ACTB	se, 5′-AGCCATGTACGTAGCCATCC-3′ as, 5′-ACCCTCATAGATGGGCACAG-3′	NM_031144	115
P450scc	se, 5′-GCGCCGGGCAGCTAGAACTT-3′ as, 5′-TGGCAGGAGGGGTGGACACG-3′	NM_017286.2	113
P450c17	se, 5′-GGCCACGCCTTTCCCTTGGT-3′ as, 5′-AGCTGGCCAGGGAGGTGCTC-3′	NM_012753.2	101
CPY19	se, 5′-CCCGGCTCTCTGGATGGATGC-3′ as, 5′-TGGCCTCAACCTCACCACGGA-3′	NM_017085.2	100

2.6. Statistical analysis

Data, expressed as mean ± SEM, were analyzed by ANOVA, followed by post-hoc comparisons with Fisher's test [33]. Morphometric data were analyzed by the Least Significant Difference test for multiple comparisons [33]. The nonparametric Mann–Whitney test was used to analyze data from tissue mRNA expression [33]. P values lower than 0.05 were considered statistically significant.

3. Results

3.1. The juvenile rat phenotype

We have previously [15] found that TP rats grow faster than CT rats after being followed up between 21 (weaning) and 30 days of age. We now found that 30-day-old TP-treated rats were significantly heavier than CT rats (Table 2). It is important to note that the gain in BW has taken place despite the lack of differences in food intake (average individual amount of food eaten per day between 21 and 30 days of age: 7.66 ± 0.59 and 6.57 ± 0.51 g/day in CT and TP rats, respectively; n = 9, P > 0.05). Interestingly, PMAT mass was greater in TP than in CT rats, even after normalizing individual pad mass by the corresponding BW (Table 2). According to a previous finding [15], the latter difference correlated well with plasma leptin concentrations, being significantly higher in TP than in CT animals (Table 2). Conversely, plasma concentrations of 17OHP4 were significantly lower in TP than in CT rats (Table 2). Ovary P450scc and CYP19 mRNA levels were significantly decreased in TP rats, whereas that of P450c17 remained the same (Table 2). Finally, no differences between groups were noticed in glucose, insulin and triglyceride peripheral levels (Table 2), nor in those of (CT and TP values, respectively) testosterone (0.24 ± 0.04 and 0.34 ± 0.06 ng/mL), E2 (29.88 ± 4.75 and 43.48 ± 14.41 pg/mL) and Cort (14.48 ± 2.49 and 12.38 ± 1.78 μg/dL).

3.2. Glomerulosa cell endocrine function in juvenile, DES-treated rats

A similar number of isolated GCs in culture displayed no group differences in spontaneous E2 release into the medium. After incubating cells with graded hCG concentrations (0.05–0.5 IU/mL), cells developed

Table 2
Parameters recorded in juvenile and adult female rats. Data are means ± SEM (n = 9 rats per group). BW: body weight; PMAT: parametrial adipose tissue; AU: arbitrary units.

	CT rats	TP rats
30 day-old		
BW (g)	53.19 ± 1.43	63.15 ± 1.32*
PMAT (mg per rat)	79.28 ± 5.74	99.29 ± 5.51*
PMAT (mg/100 g BW)	124.31 ± 7.19	150.09 ± 5.75*
Triglyceride (g/L)	0.34 ± 0.07	0.31 ± 0.04
Glucose (g/L)	1.14 ± 0.05	1.18 ± 0.04
Insulin (ng/mL)	0.56 ± 0.08	0.65 ± 0.04
Leptin (ng/mL)	1.09 ± 0.09	1.79 ± 0.14*
17OHP4 (ng/mL)	0.49 ± 0.12	0.18 ± 0.02*
Ovary P450scc (AU)	0.99 ± 0.12	0.42 ± 0.09*
Ovary P450c17 (AU)	0.98 ± 0.19	0.22 ± 0.07*
Ovary CYP19 (AU)	1.01 ± 0.16	0.14 ± 0.04*
60 day-old		
BW (g)	135.94 ± 2.77	157.14 ± 1.45*
PMAT (g per rat)	0.74 ± 0.03	1.09 ± 0.09*
PMAT (g/100 g BW)	0.51 ± 0.02	0.69 ± 0.05*
Triglyceride (g/L)	0.65 ± 0.09	0.67 ± 0.08
Glucose (g/L)	1.11 ± 0.08	1.21 ± 0.04
Insulin (ng/mL)	0.39 ± 0.05	0.84 ± 0.11*
Leptin (ng/mL)	1.32 ± 0.17	2.21 ± 0.11*
17OHP4 (ng/mL)	1.51 ± 0.39	0.13 ± 0.02*
Ovary P450scc (AU)	1.04 ± 0.19	0.37 ± 0.09*
Ovary P450c17 (AU)	1.01 ± 0.19	1.03 ± 0.24
Ovary CYP19 (AU)	1.02 ± 0.21	2.29 ± 0.11*

* P < 0.05 *vs.* CT values.

a concentration-related response (*e.g.* E2 release), regardless of the cell group examined. Although we observed only a tendency to secrete more E2 by TP GCs stimulated with 0.05 IU/mL hCG, this cell population did develop a clear hyperresponse to 0.5 IU/mL hCG stimulation (Fig. 1, upper panel). Indeed, E2 concentrations in the medium were significantly ($P < 0.05$) higher than those in the medium from CT cells.

3.3. Ovarian morphology and follicle counts in juvenile rats

Morphologically, the ovaries from CT rats exhibited follicles in various stages of development; in fact, healthy secondary, antral (tertiary) follicles and corpora lutea were observed. In contrast, the ovaries from TP rats showed small follicles in early stages of development, in addition to follicles with evidence of atresia, and antral (tertiary) follicles with a thickened granulosa layer. Fig. 1 (lower panel) shows that primary and antral (tertiary) follicle frequencies were 3- and 15-fold higher and lower, respectively ($P < 0.05$), in TP than in CT specimens, respectively. The frequencies of secondary and atretic follicles were similar in the ovaries from both studied groups.

3.4. The adult rat phenotype

Between 31 and 60 days of age, the growth curve of TP-treated rats remained displaced to the left of that depicted by CT rats (Fig. 2). Vaginal opening occurred much earlier ($P < 0.05$; $n = 9$ rats per group) in TP (13.8 ± 1.7 days) than in CT (41.4 ± 0.8 days) rats. As expected, at

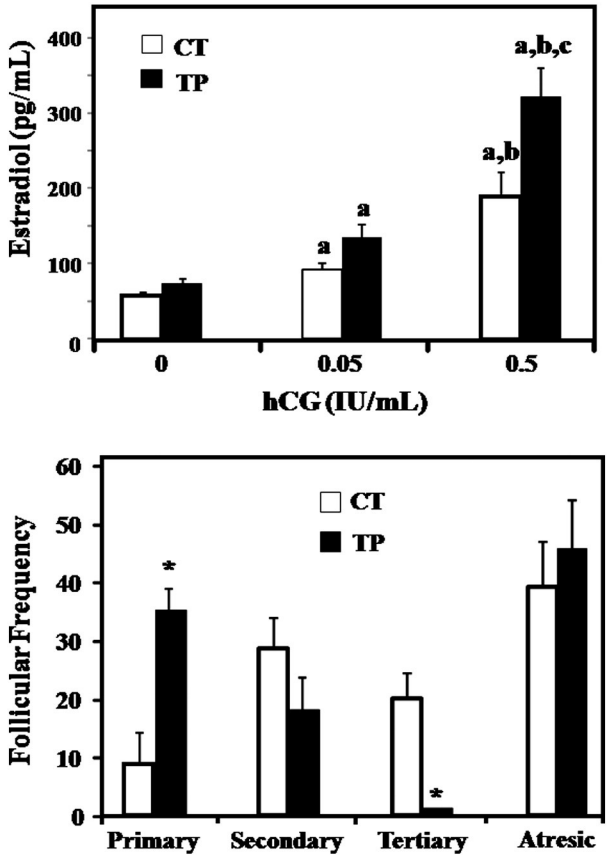

Fig. 1. Upper panel: human Chorionic Gonadotropin (hCG)-stimulated estradiol secretion by isolated ovarian granulosa cells, obtained from DES-treated, control (CT) and neonatally-androgenized (TP) juvenile rats. Values are means ± SEM ($n = 4$ different experiments, 6/7 replicates per experiment). a, $P < 0.05$ *vs.* respective basal (0 IU hCG/mL) values; b, $P < 0.05$ *vs.* 0.05 IU hCG/mL values in a similar group; c, $P < 0.05$ *vs.* CT values in the same condition. Lower panel: Follicular developmental stage of the ovaries obtained from control (CT) and neonatally-androgenized (TP) juvenile rats. Values (expressed in percentages) are means ± SEM ($n = 5$ animals per group). *$P < 0.05$ *vs.* respective CT values.

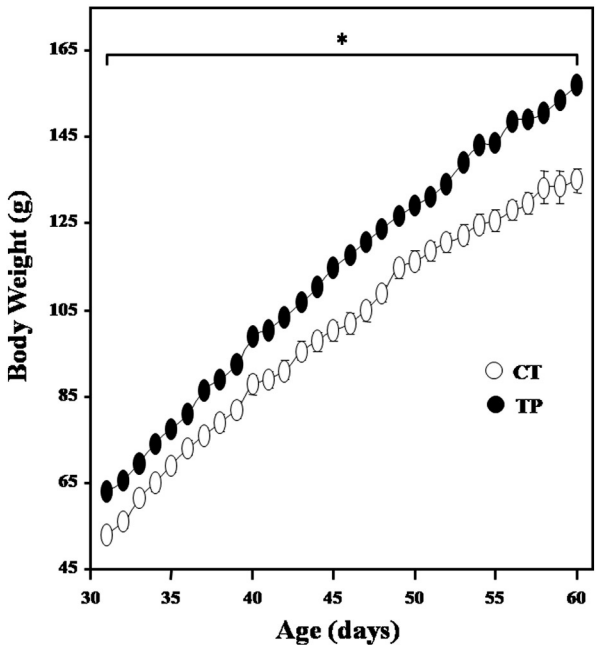

Fig. 2. Daily recorded body weight from control (CT) and neonatally-androgenized (TP) rats over development. Values are means ± SEM ($n = 12/15$ rats per group). *$P < 0.05$ *vs.* CT values.

60 days of age, TP rats were also significantly heavier than CT rats (Table 2), a fact not related to any difference in food intake (average individual amount of food eaten per day between 31 and 60 days of age: 11.87 ± 0.54 and 11.18 ± 0.57 g/day in CT and TP-treated rats, respectively; $n = 9$, $P > 0.05$). Interestingly, PMAT mass was also greater in TP than in CT rats (Table 2). Similar differences were found in plasma leptin levels, with values significantly higher in TP than in CT rats; and plasma concentrations of 17OHP4 remained significantly decreased in TP rats (Table 2). Regarding mRNA expression levels in the ovary, that of P450scc remained significantly ($P < 0.05$) lower in TP than in CT rats, whereas that of P450c17 did not differ among groups; conversely, CYP19 mRNA concentration was 2-fold higher in TP than in CT rats (Table 2). Whereas no group-differences were noticed in circulating levels of glucose and triglyceride, conversely, significantly ($P < 0.05$) higher plasma insulin values were observed in TP rats (Table 2). Finally, as occurred in juvenile individuals, no group differences were observed in circulating levels of (CT and TP values, respectively) testosterone (0.29 ± 0.05 and 0.31 ± 0.04 ng/mL), E2 (139.43 ± 21.61 and 84.76 ± 18.91 pg/mL) and Cort (9.39 ± 2.02 and 10.51 ± 2.78 μg/dL).

3.5. In vivo E2 secretion throughout an acute i.v. hCG-simulation test

Before testing, we observed that whereas regular estrous cycles characterized CT rats, TP rats showed cycles arrested at estrus. Thereafter, 60 day-old rats were subjected to i.v. hCG (5 mIU/kg BW) stimulation of E2 secretion in plasma. Results showed that basal (time zero) plasma E2 concentrations were similar in both groups and that after 1 h of hCG administration circulating levels of E2 were 2–3-fold higher ($P < 0.05$) than the respective basal values in both groups (Fig. 3, upper panel). Moreover, E2 hyper-secretion was observed in TP rats after 2 h of hCG i.v. administration (Fig. 3, upper panel).

3.6. Ovarian morphology and follicle counts in adult rats

The ovaries analyzed at 60 days of age indicated that the frequencies of secondary and atretic stage follicles were 3- and 5-fold lower and higher ($P < 0.05$) in TP than in CT rats, respectively (Fig. 3, lower panel). Conversely, no group differences were noticed in frequencies

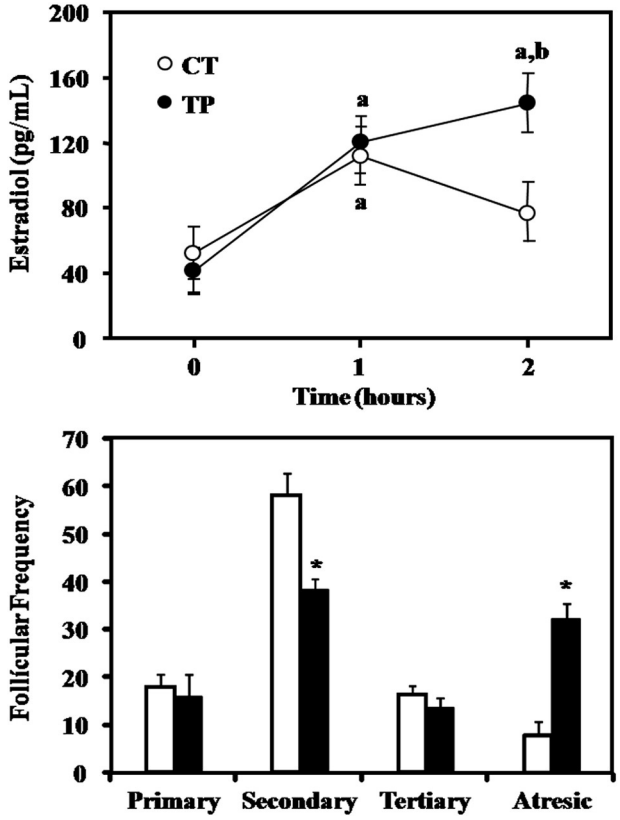

Fig. 3. Upper panel: i.v. human Chorionic Gonadotropin (hCG)-induced estradiol release in plasma, in control (CT) and neonatally-androgenized (TP) adult rats. Values are means ± SEM (n = 7/8 rats per group). a, $P < 0.05$ *vs.* respective time zero values; b, $P < 0.05$ *vs.* CT values at the same time. Lower panel: Follicular developmental stage of the ovaries obtained from control (CT) and neonatally-androgenized (TP) adult rats. Values (expressed in percentages) are means ± SEM (n = 5 animals per group). *$P < 0.05$ *vs.* respective CT values.

of both primary and antral (tertiary) follicles (Fig. 3, lower panel). Whereas ovarian images in CT animals fully correspond with expected normal characteristics (*e.g.* antral cavity, corpus luteum, ovocyte, granulosa cells and internal and external theca cells) (Fig. 4), the ovaries from TP rats displayed several dysfunctional characteristics. Indeed, images compatible with a large antral cavity in a cystic follicle bearing decreased granulosa and theca (internal and external) cell layers were observed (Fig. 4). Finally, although images corresponding to corpus luteum were observed in the ovaries from CT rats, none was seen in tissues from TP animals (data not shown).

4. Discussion

Our results confirm and extend previous data from our laboratories [1] regarding the metabolic impact of neonatal androgenization in female rats due to a single TP dose. Indeed, accelerated growth (growth curve displaced on the left) and consequent heavier body weight clearly characterized TP rats over development. Some features found in our TP rats are highly indicative of early and clear adipose tissue (AT) dysfunction, such as enlarged PMAT mass and hyperleptinemia, a phenotype found at both juvenile and adult stages. We now add a new feature of this phenotype, namely, overall impaired ovary steroidogenic function (reduced enzyme gene expression and plasma 17OHP4 levels) and follicular development.

In this TP rat model, we previously [23] found a drastic reduction in anterior pituitary (AP) LH and FSH contents (namely, at both prepubertal ages, infantile and juvenile) and failure to reach normal high circulating LH–FSH levels in infancy (15 day-old) age. It must be taken into account that the lowest AP sensitivity to LHRH in the normal rat occurs at juvenile age [7]. Thus, a relevant mechanism seems to be deeply altered in these pre-pubertal TP-treated rats: reduced gonadotropin AP store will in turn soon impair follicle maturation. In agreement with this, we now found in the ovaries of juvenile (30 day-old) TP-treated rats more primary and less antral (tertiary) follicles. This clearly indicates impaired follicular maturation, a defect probably dependent on FSH ovarian hypo-stimulation. In turn, this tissue could develop a partial reduction in the local machinery (steroidogenic enzymes) for 17OHP4 production. Interestingly, when juvenile follicles were *in vivo* induced to mature (DES-treated rats), the corresponding isolated GCs (incubated in substrate-replete medium) were fully responsive to hCG stimulation, when analyzed in terms of E2 release. In this regard, we must consider that the ovaries from our intact juvenile TP-treated rats are rich in primary follicles, although no changes in the atretic follicle population were observed.

Administration of TP to rats on postnatal day 5 did result in a rapid (12–48 h post-treatment) and transient (only up to 10 days of age) increase in ovarian androgen receptor (AR) expression [6]. Conversely, ovarian estrogen receptor (ER) expression was first (12–48 h post-treatment) reduced and later (14 days of age) restored to normal in these rats [6]. In this direction, we previously showed a selective increase in AR but not in ER or progesterone receptor in stroma and granulosa cells of primordial and primary follicles of ovine (fetal day 90) ovary at the end of TP treatment. All these data clearly suggest that AR expression level is a key step in programming adult ovarian dysfunction [16]. Moreover, increased AR expression in fetal ovaries of prenatal TP-treated sheep appears to be mediated by androgenic actions of testosterone because dihydrotestosterone, a non-aromatizable androgen, also increases AR expression in primordial/primary follicles from day-90 fetuses [16]. We must bear in mind that in rodents whole follicular differentiation is completed in early postnatal life [22], whereas in sheep this process is fully completed *in utero* [25]. Also, prenatal testosterone excess has been demonstrated to lead to reproductive dysfunctions in sheep with obesity, exaggerating these defects, accelerating follicular depletion initiated prior to puberty to stockpiling of growing follicles after puberty, a critical time point in the development of the PCOS phenotype [18].

Therefore, DNA from rodents is highly susceptible to epigenetic changes (high methylation) after a transient increase in endogenous testosterone levels, at either peri-natal or adult ages. These epigenetic changes have been observed in genes analyzed in the ovaries [34] and liver [8] from adult individuals and identified as being involved in key reproductive and metabolic functions. Moreover, these observations have served later to sustain the hypothesis that early in life androgen excess-induced epigenetic DNA modifications could be involved in the etiology of the human PCOS phenotype [34].

Upon being *in vivo* induced to rapid follicle maturation, hCG-stimulated GCs (from juvenile rats) developed normal E2 secretion. This observation allows us to postulate that retarded endogenous follicular maturation (ovary misprogramming) is a characteristic of our juvenile TP rats. However and importantly, follicular ovary ability for maturation remains unaltered (evident when appropriately stimulated with the xenoestrogen). These data are highly relevant and clearly indicative of the presence of functional GC LH receptors, probably normally or over-expressed. The follicular ovary misprogramming observed in juvenile TP rats persisted up to adulthood. Indeed, ovaries from 60 day-old TP rats showed reduced frequency of secondary follicles which correlated with enhanced frequency of atretic follicles. Moreover, whereas ovary cystic images were evident, no corpora lutea were found in adult TP-treated rats. Similar to observations of juveniles, GCs from adult TP-treated rats were fully *in vivo* responsive to i.v. hCG stimulation (*e.g.* E2 secretion). These data further suggest that the low *in vivo* steroidogenic activity found in the ovaries from TP rats could depend mainly on an early defect in AP LH/FSH production and/or secretion (*e.g.* abnormal pulsatile pattern of hormone release) [23].

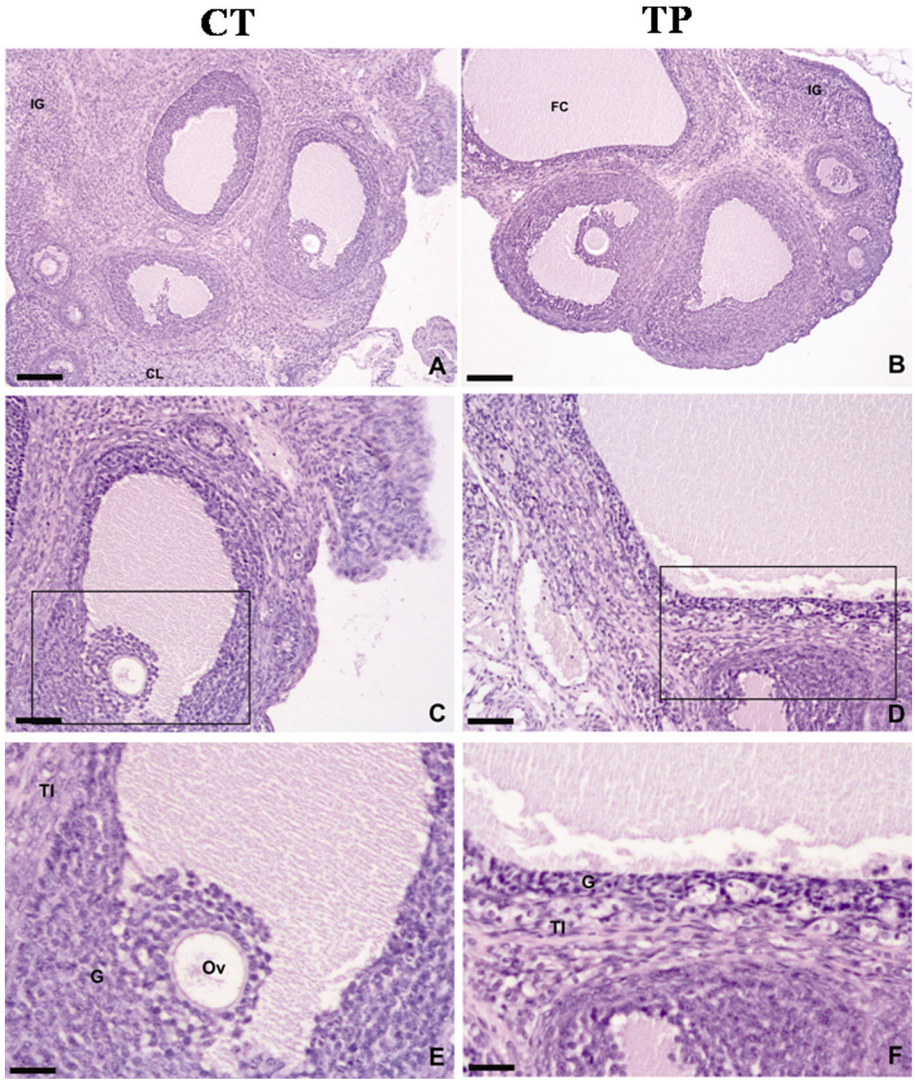

Fig. 4. Representative images of the ovaries from CT (panels A, C and E) and TP (panels B, D and F) adult rats showing ovarian structures at different magnifications: A, B: 10× (bars: 100 μm); C, D: 20× (bars: 50 μm); E, F: 40× (bars: 25 μm). CL: Corpus luteum, IG: interstitial glands; FC: follicular cyst; G: granulosa; TI: theca interna; Ov: ovocyte.

Although a large number of previous reports from several laboratories tested the effect of high androgen/estrogen dose administration at pre- and/or post-natal ages, the present study clearly supports that a single neonatal (5 day-old) administration of androgen excess is efficient enough to induce a phenotype of female rat highly resembling that of human PCOS. Indeed, the density of preantral follicles in ovary biopsies from PCOS women was reported to be six-fold higher than in those from normal women [17,29]. Moreover, PCOS women assisted for *in vitro* fertilization and embryo transfer (IVF-ET) displayed high serum E2 levels post-hCG administration (ovary GC hyperresponse) and develop a higher number of follicles, thus indicating that PCOS women are at a moderately high risk of ovarian hyperstimulation syndrome (OHSS) [12]. Consequently, the need of prior *in vitro* follicle maturation in PCOS women before IVF-ET is suggested in order to significantly reduce risk of OHSS. Furthermore, the development of insulin resistance [9] and overweight [10] are clear metabolic characteristics of the human PCOS phenotype. In this regard, we earlier addressed [1] that overall AT dysfunction in adult (100 day-old) TP rats includes high body weight, enlarged PMAT mass and adipocyte size (insulin-resistant cells that release large amounts of leptin), high circulating levels of leptin and plasminogen activator inhibitor-1 (PAI-1), and reduced adiponectin plasma concentrations. All these factors are clear aggravators [1,19,27] of AT and peripheral (as indicated here by their high insulinemia) impaired insulin sensitivity developed by TP rats. However, whether androgen excess-induced PMAT dysfunction and hyperleptinemia are responsible for inducing ovary leptin-resistance and consequently, abnormal folliculogenesis [14] remains to be determined. The present study found that, in adulthood, this TP rat model shows dysfunctions similar to those of the PCOS women phenotype, such as: a) retarded ovary follicle maturation (*e.g.* large population of preantral follicles); b) increased body and abdominal adiposity weights; and c) signs of insulin resistance. Moreover, our experimental data fully support that abnormal folliculogenesis had clearly began before puberty and lasted until adulthood. Interestingly, GCs from both juvenile and adult TP-treated rats retained full endocrine function. It remains to be determined whether androgen excess-induced epigenetic changes were installed shortly after TP administration or not, and if so, whether they are partly or fully responsible for the development of this female rat phenotype.

5. Conclusion

Our study supports that early in life transient hyperandrogenemia modifies metabolic and ovary function programming, although ovarian granulosa cells preserve their endocrine activity. Although the etiology of human PCOS is not fully understood, our data suggest that girls

with premature adrenarche produce an excess of androgen precursors that could lead to the development of a PCOS phenotype later in life, presumably through earlier hyperandrogenemia-induced epigenetic DNA changes. This condition could impact by misprogramming carbohydrate metabolism (impaired insulin sensitivity, altered glucose tolerance and Diabetes Mellitus Type 2) and, as a consequence, PCOS individuals are highly susceptible to the development of cardiovascular disease (high PAI-1 production) and reproductive dysfunction (abnormal folliculogenesis); thus resulting in sub-fertility/infertility and/or poor pregnancy outcome (early miscarriage and/or preeclampsia), even with high risk of OHSS if pregnancy is sought through IVF-ET. Therefore, appropriate pharmacological treatment, such as insulin-sensitizer combined with anti-androgen, should be considered in these women to restore full metabolic and reproductive functions.

Conflict of interest statement

The authors declare no conflict of interest.

Acknowledgements

The authors wish to thank D. Castrogiovanni and M.A. Rey for their excellent technical assistance, and S.H. Rogers for editing the manuscript. This work was supported by the Swiss FPREDM (grant 062013; to ES) and, PIP 11220120100198CO (CONICET) and PICT-2012-1415 (FONCYT) from Argentina. AG, NRS, ES and HHO are Research Career Awardees of the Argentine Council of Scientific and Technical Research (CONICET).

References

[1] A. Alzamendi, D. Castrogiovanni, H.H. Ortega, R.C. Gaillard, A. Giovambattista, E. Spinedi, Parametrial adipose tissue and metabolic dysfunctions induced by fructose-rich diet in normal and neonatal-androgenized adult female rats, Obesity (Silver Spring) 18 (2010) 441–448.
[2] R.L. Barbieri, A. Makris, R.W. Randall, G. Daniels, R.W. Kistner, K.J. Ryan, Insulin stimulates androgen accumulation in incubations of ovarian stroma obtained from women with hyperandrogenism, J. Clin. Endocrinol. Metab. 62 (1986) 904–910.
[3] R.L. Barbieri, S. Smith, K.J. Ryan, The role of hyperinsulinemia in the pathogenesis of ovarian hyperandrogenism, Fertil. Steril. 50 (1988) 197–212.
[4] C.A. Barraclough, R.A. Gorski, Evidence that the hypothalamus is responsible for androgen-induced sterility in the female rat, Endocrinology 68 (1961) 68–79.
[5] K.L. Britt, A.E. Drummond, V.A. Cox, M. Dyson, N.G. Wreford, M.E. Jones, et al., An age-related ovarian phenotype in mice with targeted disruption of the cyp 19 (aromatase) gene, Endocrinology 141 (2000) 2614–2623.
[6] A. Bukovsky, M.E. Ayala, R. Dominguez, J.A. Keenan, J. Wimalasena, R.F. Elder, et al., Changes of ovarian interstitial cell hormone receptors and behavior of resident mesenchymal cells in developing and adult rats with steroid-induced sterility, Steroids 67 (2002) 277–289.
[7] A. Castro-Vazquez, S.R. Ojeda, Changes in pituitary responsiveness to LH–RH during puberty in the female rat: initiation of the priming effect, Neuroendocrinology 23 (1977) 88–98.
[8] M.A. Dkhil, S. Al-Quraishy, A.A. Abdel-Baki, F. Ghanjati, M.J. Arauzo-Bravo, D. Delic, F. Wunderlich, Epigenetic modifications of gene promoter DNA in the liver of adult female mice masculinized by testosterone, J. Steroid Biochem. Mol. Biol. 145 (2015) 121–130.
[9] A. Dunaif, Hyperandrogenic anovulation (PCOS): a unique disorder of insulin action associated with an increased risk of non-insulin-dependent diabetes mellitus, Am. J. Med 98 (1995) 33S–39S.
[10] A. Dunaif, M. Graf, J. Mandeli, V. Laumas, A. Dobrjansky, Characterization of groups of hyperandrogenic women with acanthosis nigricans, impaired glucose tolerance, and/or hyperinsulinemia, J. Clin. Endocrinol. Metab. 65 (1987) 499–507.
[11] A. Dunaif, X. Wu, A. Lee, E. Diamanti-Kandarakis, Defects in insulin receptor signaling in vivo in the polycystic ovary syndrome (PCOS), Am. J. Physiol. Endocrinol. Metab. 281 (2001) E392–E399.
[12] M.J. MacDougall, S.L. Tan, A. Balen, H.S. Jacobs, A controlled study comparing patients with and without polycystic ovaries undergoing in-vitro fertilization, Hum. Reprod. 8 (1993) 233–237.
[13] F. Nobels, D. Dewailly, Puberty and polycystic ovarian syndrome: the insulin/insulin-like growth factor I hypothesis, Fertil. Steril. 58 (1992) 655–666.
[14] M.O. Olatinwo, G.K. Bhat, C.D. Stah, D.R. Mann, Impact of gonadotropin administration on folliculogenesis in prepubertal ob/ob mice, Mol. Cell. Endocrinol. 245 (2005) 121–127.
[15] L. Ongaro, A. Giovambattista, E. Spinedi, Impact of neonatal manipulation of androgen receptor function on endocrine–metabolic programming in the juvenile female rat, ISRN Endocrinol. 181950 (2013) 1–7.
[16] H.H. Ortega, N.R. Salvetti, V. Padmanabhan, Developmental programming: prenatal androgen excess disrupts ovarian steroid receptor balance, Reproduction 137 (2009) 865–877.
[17] V. Padmanabhan, A. Veiga-Lopez, Developmental origin of reproductive and metabolic dysfunctions: androgenic versus estrogenic reprogramming, Semin. Reprod. Med. 29 (2011) 173–186.
[18] V. Padmanabhan, P. Smith, A. Veiga-Lopez, Developmental programming: impact of prenatal testosterone treatment and postnatal obesity on ovarian follicular dynamics, J. Dev. Orig. Health Dis. 3 (2012) 276–286.
[19] M. Perelló, D. Castrogiovanni, G. Moreno, R.C. Gaillard, E. Spinedi, Neonatal hypothalamic androgenization in the female rat induces changes in peripheral insulin sensitivity and adiposity function at adulthood, Neuroendocrinol. Lett. 24 (2003) 241–248.
[20] M. Perelló, D. Castrogiovanni, A. Giovambattista, R.C. Gaillard, E. Spinedi, Impairment in insulin sensitivity after early androgenization in the post-pubertal female rat, Life Sci. 80 (2007) 1792–1798.
[21] T. Sir-Petermann, V. Piwonka, F. Pérez, M. Maliqueo, S.E. Recabarren, L. Wildt, Are circulating leptin and luteinizing hormone synchronized in patients with polycystic ovary syndrome? Hum. Reprod. 14 (1999) 1435–1439.
[22] T.A. Sokka, T.M. Hämäläinen, A. Kaipia, D.W. Warren, I.T. Huhtaniemi, Development of luteinizing hormone action in the perinatal rat ovary, Biol. Reprod. 55 (1996) 663–670.
[23] E. Spinedi, V. Mariani, M. Bulfon, M. Colombani-Vidal, H. Scaglia, Analysis of the hypothalamic–pituitary–ovary axis in the neonatally-androgenized female rat, J. Endocrinol. Investig. 13 (1990) 481–488.
[24] V. Tyndall, M. Broyde, R. Sharpe, M. Welsh, A.J. Drake, A.S. McNeilly, Effect of androgen treatment during foetal and/or neonatal life on ovarian function in prepubertal and adult rats, Reproduction 143 (2012) 21–33.
[25] A. Veiga-Lopez, W. Ye, D.J. Phillips, C. Herkimer, P.G. Knight, V. Padmanabhan, Developmental programming: deficits in reproductive hormone dynamics and ovulatory outcomes in prenatal, testosterone-treated sheep, Biol. Reprod. 78 (2008) 636–647.
[26] A.M. Vitale, O.M. Gonzalez, F. Parborell, G. Hirsuta, S. Campo, M. Tesone, Inhibin a increases apoptosis in early ovarian antral follicles of diethylstilbestrol-treated rats, Biol. Reprod. 67 (2002) 1989–1995.
[27] K. Walder, A. Filippis, S. Clark, P. Zimmet, G.R. Collier, Leptin inhibits insulin binding in isolated rat adipocytes, J. Endocrinol. 155 (1997) R5–R7.
[28] K.A. Walters, C.M. Allan, D.J. Handelsman, Androgen actions and the ovary, Biol. Reprod. 78 (2008) 380–389.
[29] L.J. Webber, S. Stubbs, J. Stark, G.H. Trew, R. Margara, R. Hardy, S. Franks, Formation and early development of follicles in the polycystic ovary, Lancet 362 (2003) 1017–1021.
[30] P.M. Wise, N. Rance, M. Selmanoff, C.A. Barraclough, Changes in radioimmunoassayable luteinizing hormone-releasing hormone in discrete brain areas of the rat at various times on proestrus, diestrous day 1, and after phenobarbital administration, Endocrinology 108 (1981) 2179–2185.
[31] T.K. Woodruff, R.J. Lyon, S.E. Hansen, G.C. Rice, J.P. Mather, Inhibin and activin locally regulate rat ovarian folliculogenesis, Endocrinology 127 (1990) 3196–3205.
[32] R.J. Zachow, D.A. Magoffin, Direct intraovarian effects of leptin: impairment of the synergistic action of insulin-like growth factor–I on follicle-stimulating hormone-dependent estradiol-17 beta production by rat ovarian granulosa cells, Endocrinology 138 (1997) 847–850.
[33] J. Zar, Biostatistical analysis, Prentice-Hall Inc., Englewood Cliffs, New Jersey, 1970.
[34] D. Zhang, J. Cong, H. Shen, Q. Wu, X. Wu, Genome-wide identification of aberrantly methylated promoters in ovarian tissue of prenatally androgenized rats, Fertil. Steril. 102 (2014) 1458–1467.